

Phenomenological description of the γ^*p cross section at low Q^2

A. Rostovtsev¹, M.G. Ryskin², and R. Engel³

- ¹ ITEP, B. Chermushkinskaja 25, Moscow 117259, Russia
- ² Petersburg Nuclear Physics Institute, 188350, Gatchina, St. Petersburg, Russia.
- ³ Univ. of Delaware, Bartol Res. Inst., Newark DE 19716, USA.

Abstract

Low Q^2 photon-proton cross sections are analysed using a simple, QCD-motivated parametrisation $\sigma_{\gamma^*p} \propto 1/(Q^2 + Q_0^2)$, which gives a good description of the data. The Q^2 dependence of the γ^*p cross section is discussed in terms of the partonic transverse momenta of the hadronic state the photon fluctuates into.

1 Introduction

Traditionally photoproduction and DIS are considered as processes which are governed by different underlying physics. Whereas most of the features of DIS processes can be described in terms of perturbative QCD, photoproduction is dominated by non-perturbative effects. This point of view seems to be justified by the Q^2 dependence of the γ^*p cross section which exhibits a clearly visible transition region between photoproduction and DIS at about $Q^2 \sim 0.5\text{GeV}^2$. On the other hand, the steady transition from photoproduction to DIS highlights the importance of obtaining a description which smoothly links the non-perturbative and perturbative domains, see for example [1–6].

There exist now high precision deep inelastic lepton scattering data [7–11] covering both the low Q^2 and high Q^2 domains, as well as measurements of the photoproduction cross section [12–14]. In the present paper we discuss a simple QCD-motivated parametrisation of the observed Q^2 dependence of the γ^*p cross section, which is closely related the average transverse momentum of secondary particles produced in the photon hemisphere. In addition, the question of the hard scale in deep-inelastic scattering is discussed within the framework of k_T factorization.

2 Theoretical framework of k_t factorization

Let $\sigma_{\gamma^*p}(s, Q^2)$ be the total cross section for the process $\gamma^*p \rightarrow X$ where Q^2 is the virtuality of the photon and \sqrt{s} is the γ^*p centre-of-mass energy. For $s \gg Q^2$ the $\gamma^* \rightarrow q\bar{q}$ fluctuations occur over a much longer time scale than the interaction of the $q\bar{q}$ pair with the target proton. Therefore the γ^*p cross section is well approximated by the probability $|\mathcal{M}|^2$ of the $\gamma^* \rightarrow q\bar{q}$ transition multiplied by the imaginary part of the forward amplitude describing the $q\bar{q}$ -proton interaction

$$\Im m(A_{q\bar{q}+p}) = s\sigma_{q\bar{q}+p}, \quad (1)$$

where $\sigma_{q\bar{q}+p}$ is the cross section for the scattering of the $q\bar{q}$ system on the proton. For transversely polarized photons the amplitude of the $\gamma^* \rightarrow q\bar{q}$ transition reads

$$\mathcal{M}_T = \frac{\sqrt{z(1-z)}}{\bar{Q}^2 + k_T^2} \bar{u}_\lambda(\gamma \cdot \epsilon_\pm) u_{\lambda'} = \frac{(\epsilon_\pm \cdot k_T)[(1-2z)\lambda \pm 1]\delta_{\lambda, -\lambda'} + \lambda m_q \delta_{\lambda\lambda'}}{\bar{Q}^2 + k_T^2}, \quad (2)$$

where the q and \bar{q} longitudinal momentum fractions and transverse momenta are z , \vec{k}_t and $(1-z)$, $-\vec{k}_t$ respectively. We use the notation of Ref. [15], which is based on the earlier work of Ref. [16, 17]. Namely \bar{Q}^2 and the photon polarization vectors are given by

$$\bar{Q}^2 = z(1-z)Q^2 + m_q^2 \quad (3)$$

$$\epsilon_T = \epsilon_\pm = \frac{1}{\sqrt{2}}(0, 0, 1, \pm i), \quad (4)$$

and where $\lambda, \lambda' = \pm 1$ according to whether the q, \bar{q} helicities are $\pm \frac{1}{2}$.

In terms of the quark momentum variables we thus obtain

$$\sigma_{\gamma_T^* p}(s, Q^2) = \sum_q \alpha \frac{e_q^2}{2\pi} \int dz dk_T^2 \frac{[z^2 + (1-z)^2]k_T^2 + m_q^2}{(Q^2 + k_T^2)^2} N_c \sigma_{q\bar{q}+p}(s, k_T^2) \quad (5)$$

where the number of colours $N_c = 3$.

Eq. (5) can be rewritten as a dispersion relation in M^2 , with M being the invariant mass of the $q\bar{q}$ pair. With

$$M^2 = \frac{k_T^2 + m_q^2}{z(1-z)} \quad (6)$$

and a change of the integration variable from dk_T^2 to dM^2 one gets¹

$$\sigma_{\gamma_T^* p}(s, Q^2) = \frac{\alpha}{2\pi} \sum_q e_q^2 \int dz \frac{dM^2}{(Q^2 + M^2)^2} \{M^2 [z^2 + (1-z)^2] + 2m_q^2\} N_c \sigma_{q\bar{q}+p}(s, k_T^2). \quad (7)$$

This can be compared with the corresponding expression of the generalized vector dominance model [18–20]

$$\sigma_{\gamma_T^* p}(s, Q^2) = \sum_q \int_0^\infty \frac{dM^2}{(Q^2 + M^2)^2} \rho(M^2) \sigma_{q\bar{q}+p}(s, M^2), \quad (8)$$

where the spectral function ρ represents the density of $q\bar{q}$ states. A similar dispersion relation has been used, for example, in [21, 22] to describe the structure function F_2 over the full Q^2 range. In comparison to (8) we see that (7) is a two-dimensional integral. To see the reason for this let us consider massless quarks. Then $z = \frac{1}{2}(1 + \cos \theta)$ where θ is the angle between the q and the γ^* in the $q\bar{q}$ rest frame. The dz integration is implicit in (8) as the integration over the quark angular distribution in the spectral function ρ .

At first sight the Q^2 dependence of the cross section (8) should be $\sigma_{\gamma^* p} \propto 1/(Q^2 + M_0^2)^2$. This is true if one deals with only one vector meson or when the dominant contribution in (8) comes from a limited range of M^2 . On the other hand when all the possible values of M^2 are taken into account the result is

$$\sigma_{\gamma^* p} \propto \int \frac{dM^2}{(Q^2 + M^2)^2} = \frac{1}{Q^2 + M_0^2}. \quad (9)$$

Just such a behaviour is expected in our approach (see Sect. 3 and Eq. (18)).

To obtain a complete description of the $\gamma^* p$ cross section a deed model for the $q\bar{q}$ -proton interaction is needed. Such a model is developed, for example, in [23]. Furthermore, longitudinally polarized photons have to be considered. However for our phenomenological discussion it is sufficient to investigate some general features of (5).

¹ Of course, in principle, there may be non-diagonal elements of the amplitude $A_{q\bar{q}+p}$ of (1). However it is known, both from experiment and from triple Regge theory, that such non-diagonal transitions are suppressed in the forward direction. In terms of the additive quark model the suppression is the result of the orthogonality of the initial and final wave functions for a non-diagonal transition.

3 Virtuality dependence

The Q^2 dependence in Eq. (5) comes mainly from the two quark propagators $1/(\bar{Q}^2 + k_T^2)^2 = 1/(z(1-z)Q^2 + k_T^2)^2$ where in the r.h.s. of the last equality we neglect the small quark mass (m_q^2) in the \bar{Q}^2 term. In order to demonstrate the expected Q^2 behaviour of the cross section (5) let us first write the expression in the simplified form

$$\sigma_{\gamma_T^* p}(Q^2) \propto \int_0^1 dz \frac{dz}{(zQ^2 + k_T^2)^2} \quad (10)$$

and perform the dz integration. It gives the result

$$\sigma_{\gamma_T^* p}(Q^2) \propto \frac{1}{k_T^2(Q^2 + 2k_T^2)} \propto \frac{1}{Q^2 + 2k_T^2}. \quad (11)$$

It can be checked by explicit numerical integration that the z dependent part of the integral (5)

$$J_\sigma = \int_0^1 dz \frac{[z^2 + (1-z)^2]}{(z(1-z)Q^2 + k_T^2)^2} \quad (12)$$

is well approximated by

$$J_{\text{app.}} = \frac{2}{k_T^2(Q^2 + 3k_T^2)}. \quad (13)$$

The ratio $r = J_\sigma/J_{\text{app.}}$ tends to 1 in the asymptotic limits $Q^2 \rightarrow 0$ or $Q^2 \rightarrow \infty$ and reaches a minimum of about 0.96 at $Q^2 \sim 8k_T^2$.

Using this approximation (5) can be written as

$$\begin{aligned} \sigma_{\gamma_T^* p}(s, Q^2) &= N_c \alpha \sum_q \frac{e_q^2}{2\pi} \int d \log(k_T^2) \frac{2}{Q^2 + 3k_T^2} k_T^2 \sigma_{q\bar{q}+p}(s, k_T^2) \\ &\propto N_c \alpha \sum_q \frac{e_q^2}{2\pi} \frac{2}{Q^2 + 3\overline{k_T^2}} \overline{k_T^2} \sigma_{q\bar{q}+p}(s, \overline{k_T^2}), \end{aligned} \quad (14)$$

where $\overline{k_T^2}$ is the characteristic transverse momentum of the quark. In Eq. (14) the Q^2 dependence is almost factorised and is mainly given just by the factor $1/(Q^2 + 3\overline{k_T^2})$.

Now let us discuss the structure of the integral (14) over dk_T^2 . Of course the large distances, i.e. very small $k_T < 1/r$ (where $r \sim R_N$ is of the order of nucleon radius R_N) are suppressed by the confinement. At very large $k_T \gg 1/r$ based on the perturbative QCD and neglecting the anomalous dimension one expects the cross section $\sigma_{q\bar{q}+p} \propto 1/k_T^2$. Thus in the ultraviolet region (at $k_T^2 > Q^2$) the integral (14) is convergent.

The main contribution comes from the mediate (more or less soft) $k_T^2 \sim 0.1 - 0.4 \text{ GeV}^2$ interval. Typically the cross section is large in the soft region, where it falls down with k_T exponentially; then at $k_T > 1 - 3 \text{ GeV}$ (corresponding to a small distances) it has the power-like tail .

Note that the predicted behaviour

$$\sigma_{\gamma^*p} \propto \frac{1}{Q^2 + 3\overline{k_T^2}} \quad (15)$$

does not depend too much on concrete form of the $q\bar{q}$ cross section.

As an extreme example let us consider a simple "soft" approximation

$$\sigma_{q\bar{q}+p}(s, k_T^2) = \sigma_0(s)\Theta(k_T^2 - \mu^2)\Theta(\overline{K_T^2} - k_T^2) \quad (16)$$

which corresponds to soft scattering where the quark-proton cross section is saturated for $\mu^2 < k_T^2 < \overline{K_T^2}$ and vanishes everywhere else. Then the γ^*p cross section reads

$$\sigma_{\gamma_T^*p}(s, Q^2) \propto \sigma_0(s) \ln \left(\frac{Q^2 + 3\overline{K_T^2}}{Q^2 + 3\mu^2} \right) . \quad (17)$$

Despite of the fact that (17) takes now a logarithmic form for the numerical values for $\overline{K_T^2}$ discussed in the following (17) predicts almost the same Q^2 behaviour (15) as Eq. (14).

One has to expect also that the characteristic value $\overline{k_T^2}$ should increase with energy. For larger collision energies the evolution chain (which produces finally the wee parton) becomes longer. At each step of evolution a new parton is emitted and the active parton gets some extra transverse momentum. Therefore, as in the case of multiple small angle scattering in a thick target, the final 'intrinsic' k_T of the active parton grows with the number of interactions (the number of evolution steps). In the framework of perturbative QCD this growth is originated in the summation of the double logarithmic contributions of the type $(\alpha_s \log(k_T^2) \log(s))^n$ and is described in terms of the anomalous dimensions. Due to the larger value of anomalous dimension γ at higher energies one expects the larger characteristic value $\overline{k_T^2}$.

Finally we will neglect the weak logarithmic Q^2 dependence of $\overline{k_T^2}$ in (14,15) (which is, of course, not excluded completely) and try to describe the data with the parametrisation

$$\sigma_T(\gamma^*p) \propto \frac{1}{Q^2 + Q_0^2} \quad (18)$$

using Q_0^2 given by the characteristic value $\overline{k_T^2}$ of the quark transverse momentum

$$Q_0^2 \approx 3\overline{k_T^2} . \quad (19)$$

The value of Q_0^2 becomes unimportant for large Q^2 so we use the value of $\overline{k_T^2}$ as determined at small Q^2 (say, in photoproduction at $Q^2 = 0$).

Since the integral (14) over k_T^2 has a logarithmic structure one can not estimate the characteristic value of $\overline{k_T^2}$ through the average of k_T^2 . Multiplying the integrand by an extra power of k_T^2 destroys the whole structure of the integral and enlarges crucially the essential values of k_T^2 . Therefore we estimate $\overline{k_T^2}$ by averaging the logarithm of the squared transverse momentum

$$\overline{k_T^2} = \exp \left(\langle \log(k_T^2) \rangle \right) . \quad (20)$$

Of course, one cannot measure directly k_T^2 of a quark. So we have to relate the k_T of the quark jet to the transverse momenta p_T of secondary hadrons in the photon fragmentation region. Contrary to the large E_T jet fragmentation here (for not too large k_T) the value of p_T is not so small in comparison with k_T . If one assumes that in photoproduction both values (k_T of the quark and p_T of secondary hadrons) are controlled by the typical temperature T then we may expect that our $\overline{k_T^2}$ is close (or equal) to the average $\overline{p_T^2}$ of secondary hadrons (in the photon fragmentation region).

To understand better the relation between the values of $\overline{k_T^2}$ and $\overline{p_T^2}$ we use a standard Monte Carlo program which is in agreement with fixed target and HERA photoproduction data, in particular with the measured transverse is momentum spectra of secondaries. The corresponding predictions for the PHOJET (which, of course is not excluded completely) event generator [24] are given in Tab. 1 for two energies at which inclusive transverse momentum distributions of secondaries have been measured [25–27]. Indeed for the photon fragmentation region ($x_F > 0.2$) the $\overline{p_T^2}$ of secondary hadrons in non-diffractive events is close to the parton $\overline{k_T^2}$ and increases with energy. A similar increase of the $\overline{p_T^2}$ of secondary hadrons with the collision energy was observed experimentally in deep inelastic scattering [28–30].

Table 1: Logarithmic average transverse momenta of partons (k_T) and charged final state hadrons (p_T) produced in non-diffractive γp collisions in a photon fragmentation ($x_F > 0.2$) region as predicted by the PHOJET event generator [24]. In the last column the Q_0^2 values as obtained by a fit to photoproduction and DIS data are given.

\sqrt{s} (GeV)	$\overline{k_T^2}$ (GeV ²)	$\overline{p_T^2}$ (GeV ²)	Q_0^2 (GeV ²)
15	0.19	0.17	0.42 ± 0.01
200	0.5	0.35	1.04 ± 0.04

In Fig. 1 the parametrisation (18) is compared to photoproduction [13,14] and DIS [7–9] data at two different energies ($\sqrt{s} = 200$ GeV and $\sqrt{s} = 15$ GeV). To obtain the total virtual photon–proton cross sections we use $\sigma_{\gamma^*p} = (4\pi\alpha/Q^2)F_2(x, Q^2)$. Where necessary, the measured values of $F_2(x, Q^2)$ have been interpolated using a smooth function. The overall normalization uncertainties have been neglected in the fit of the data in the Fig. 1.

The measured total photon–proton cross sections are fitted to the parametrisation (18) with only two free parameters: Q_0^2 and an overall normalization for each of the two sets of the data. The results of the fit are also presented in Fig. 1 as lines. We can conclude that (14,18) reproduce all the main features of the data (including the photoproduction points) in a wide range of energies and Q^2 . As expected, the parameter Q_0^2 is energy dependent. It’s value is 1.04 ± 0.04 GeV² at $\sqrt{s} = 200$ GeV while for $\sqrt{s} = 15$ GeV we needed $Q_0^2 = 0.42 \pm 0.01$ GeV². Relating the experimentally measured transverse momentum spectrum to the parameter $\overline{k_T^2}$,

the increase of $\overline{k_T^2}$ from the energies of fixed target experiments to the HERA kinematic region agrees well the rise of Q_0^2 parameter obtained above (see Eq. (19)).

It is known that in the small- x region the DGLAP evolution leads to a strong scaling violation which reveals itself in a rather large positive value of the anomalous dimension. Therefore, at large energies the Q^2 behaviour of the cross section $\sigma \propto 1/(Q^2)^{1-\gamma}$ becomes more flat. In our parametrisation (18) the same effect is hidden in the value of $Q_0^2 \propto k_T^2$. Due to a rather large anomalous dimension and $\sigma_{q\bar{q}+p}(s, k_T^2) \propto 1/(k_T^2)^{1-\gamma}$, the essential values of k_T^2 increase with energy faster than $\log(s)$. Consequently, the Q^2 distribution becomes broader.

The expression (18) fits also quite well the data on the nuclear targets. In Fig. 2 the parametrisation (18) is compared to the available photoproduction [14] and DIS [10, 11] data at energy $\sqrt{s} = 10$ GeV for the nucleon in deuteron, carbon and calcium nuclei. The value of Q_0^2 increases with the atomic number A but the normalization factors are the same within the errors. In other words not only the anomalous dimension behaviour of DIS cross section but the effect of shadowing is absorbed in the value of Q_0^2 (to be more precise – in the A -dependence of Q_0^2) as well.

What is the origin of A -dependence of Q_0^2 ? From the point of view of the photon-quark interaction the k_T in Eq. (14) plays the role of the intrinsic transverse momentum of the quarks. So we have to discuss the parton wave function of the nucleon/nuclear target. Note that in coordinate space the longitudinal interval occupied by the small- x wee parton $z \sim 1/m_N x$ (m_N is the nucleon mass) increases with $1/x$ and for $x < 0.1 - 0.2$ the partons originated by different nucleons start to overlap and interact with each other. This parton-parton rescattering leads to the well-known shadowing effects. However a quark can not disappear completely since it carries conserved quantum numbers (i.e. charge, isospin, etc.). The only possibility is to move the quark from the densely populated phase space region to another one. Consequently the rescattering mainly enlarges the transverse momentum and pushes the quark out of the small k_T region.

Therefore we have to expect a larger value of $Q_0^2 = 3\overline{k_T^2}$ for a heavier nuclei. To estimate the size of this effect let us consider soft rescattering. With a quark-nucleon cross section of $\sigma_{qN} \simeq \frac{1}{3}\sigma_{NN} \simeq 10 - 15$ mb the mean number of quark interactions in Ca will be $\nu_q \sim 0.7 - 1$. Each soft rescattering increases the value of $\overline{k_T^2}$ by about $\Delta k^2 \sim (0.3 - 0.4 \text{ GeV})^2$ since $k_A^2 \approx \overline{k_T^2} + \nu_q \cdot \Delta k^2$. The parameter Q_0^2 for Ca should be of about $3\nu_q \cdot \Delta k^2 \sim 0.3 - 0.4 \text{ GeV}^2$ larger than for a free nucleon target. This is in good agreement with the fit results given in Tab. 2.

The same parton-parton rescattering may explain at least part of the growth of Q_0^2 with the energy; due to the fact that at large energies (small x) the parton density increases and even in the case of a single proton the parton-parton interaction becomes not negligible.

In terms of the dispersion relation (8) one can say that in dense matter (heavy nuclei or large \sqrt{s}) the effective mass (M^2) of $q\bar{q}$ -pair increases. The point-like (large M^2) configurations with a small cross section which penetrate a thin target without any interaction are absorbed by a dense target and give an essential contribution to the cross section.

Table 2: Fit results for the parameter Q_0^2 for different energies and targets. The data sets have been interpolated to the given energy.

\sqrt{s} (GeV)	target	Q_0^2 (GeV ²)	data used
200	p	1.04 ± 0.04	H1, ZEUS
100	p	0.75 ± 0.04	H1, ZEUS
15	p	0.42 ± 0.01	E665
10	d	0.46 ± 0.02	E665
10	d	0.44 ± 0.03	EMC
10	C	0.56 ± 0.06	EMC
10	Ca	0.76 ± 0.08	EMC

4 Conclusive remarks

At low x photon–proton scattering can be understood as the fluctuation of the virtual photon into a hadronic state and the subsequent scattering of this state on the proton. We have shown that cross section data on fixed target and HERA deep-inelastic scattering support this interpretation.

On this basis, a simple parametrisation of the Q^2 dependence of the γ^*p cross section has been derived. The essential parameter Q_0^2 of this parametrisation can be estimated from the measurement of secondaries produced in the photon fragmentation region.

This data analysis also confirms the prediction of the k_T factorization approximation that the hard scale of the process is not the initial photon virtuality Q^2 but the parton k_T of the hadronic fluctuation. Of course, the essential values of k_T^2 are correlated with Q^2 but neither directly equal nor proportional to Q^2 . Instead, the correlation between k_T^2 and Q^2 is rather broad. Therefore, in order to fix the hard scale of the deep-inelastic process it is better to use the transverse energy (E_T) measurements in the photon fragmentation region, than the value of the colliding photon virtuality. Fixing the hard scale by high p_T secondary hadrons from the photon fragmentation region instead of the photon virtuality Q^2 , a faster transition to hard scattering has been observed [31].

Finally, we may say that the cross section fits presented in this work suggest that low- x deep inelastic scattering is characterized by rather "soft" (corresponding to $k_T^2 \sim 0.15 - 0.3$ GeV²) quark-nucleon ($\sigma_{q\bar{q}+p}$) interactions.

Acknowledgements

MGR thanks the INTAS (95-311) and the Russian Fund of Fundamental Research (98-02-17629) for support. One of the authors (RE) is supported by the U.S. Department of Energy under grant DE-FG02-91ER40626. AR gratefully acknowledge the University of Antwerpen for support.

References

- [1] A. Levy: The transition from the photoproduction to the DIS region, TAUP 2349-96, (hep-ex/9608009), 1996
- [2] A. Capella, A. Kaidalov, C. Merino and J. Trân Thanh Vân: Phys. Lett. B337 (1994) 358
- [3] D. Schildknecht and H. Spiesberger: Generalized vector dominance and low x inelastic electron - proton scattering, BI-TP-97-25, (hep-ph/9707447), 1997
- [4] P. Desgrolard, L. Jenkovszky and F. Paccanono: Interpolating between soft and hard dynamics in deep inelastic scattering, LYCEN-9808, (hep-ph/9803286), 1998
- [5] P. V. Landshoff and A. Donnachie: Small x : two pomerons!, DAMTP-98-34, (hep-ph/9806344), 1998
- [6] B. Povh: Hadron interactions: hadron sizes, MPIH-V21-1998, talk given at 14th Winter Workshop on Nuclear Dynamics, Snowbird, UT, 31 Jan - 7 Feb 1998, (hep-ph/9806344), 1998
- [7] H1 Collab.: S. Aid et al.: Nucl. Phys. B470 (1996) 3
- [8] H1 Collab.: C. Adloff et al.: Nucl. Phys. B497 (1997) 3
- [9] ZEUS Collab.: J. Breitweg et al.: Phys. Lett. B407 (1997) 432
- [10] E665 Collab.: M. R. Adams et al.: Phys. Rev. D54 (1996) 3006
- [11] EMC Collab.: M. Arneodo et al.: Nucl. Phys. B333 (1989) 1
- [12] ZEUS Collab.: M. Derrick et al.: Phys. Lett. B293 (1992) 465
- [13] H1 Collab.: S. Aid et al.: Z. Phys. C69 (1995) 27
- [14] H. Schopper (ed.): *Total Cross-Sections for Reactions of High Energy Particles* Landolt-Börnstein, New Series, Vol. I/12b Springer, Berlin 1987
- [15] E. M. Levin, A. D. Martin, M. G. Ryskin and T. Teubner: Z. Phys. C74 (1997) 671
- [16] A. H. Mueller: Nucl. Phys. B335 (1990) 115
- [17] S. J. Brodsky and P. Lepage: Phys. Rev. D22 (1980) 2157
- [18] J. J. Sakurai and D. Schildknecht: Phys. Lett. 40B (1972) 121
- [19] J. J. Sakurai and D. Schildknecht: Phys. Lett. 41B (1972) 489

- [20] A. Donnachie and G. Shaw: *Generalized Vector Dominance*, Plenum Press, New York, 1978 in: *Electromagnetic Interactions of Hadrons, Volume 2*, ed. by A. Donnachie and G. Shaw, p. 169
- [21] B. Badelek and J. Kwieciński: *Phys. Lett.* B295 (1992) 263
- [22] J. Kwieciński and B. Badelek: *Z. Phys.* C43 (1989) 251
- [23] A. D. Martin, M. G. Ryskin and A. M. Stasto: The description of F_2 at low Q^2 , DTP/98/20, (hep-ph/9806212), 1998
- [24] R. Engel and J. Ranft: *Phys. Rev.* D54 (1996) 4244
- [25] OMEGA Photon Collab.: R. J. Apsimon et al.: *Z. Phys.* C43 (1989) 63
- [26] H1 Collab.: I. Abt et al.: *Phys. Lett.* B328 (1994) 177
- [27] ZEUS Collab.: M. Derrick et al.: *Z. Phys.* C67 (1995) 227
- [28] ZEUS Collab.: M. Derrick et al.: *Z. Phys.* C70 (1996) 1
- [29] EMC Collab.: J. Ashman et al.: *Z. Phys.* C52 (1991) 361
- [30] E665 Collab.: M. R. Adams et al.: *Phys. Lett.* B272 (1991) 163
- [31] H1 Collab.: S. Aid et al.: *Phys. Lett.* B392 (1997) 234

Figure Captions.

Figure 1: Total γp cross section as function of $Q^2 + Q_0^2$. The filled circles represent HERA deep inelastic data at $W = 200$ GeV, triangles show the data from E665 experiment at $W = 15$ GeV, the squares represent the photoproduction measurements at corresponding energies.

Figure 2: Total cross section of photon–nucleon interaction as function of $Q^2 + Q_0^2$ at $W = 10$ GeV. The filled circles represent EMC data on μd , μC , and μCa deep inelastic scattering, triangles show the μd data from E665 experiment, the squares represent the photoproduction γd measurement.

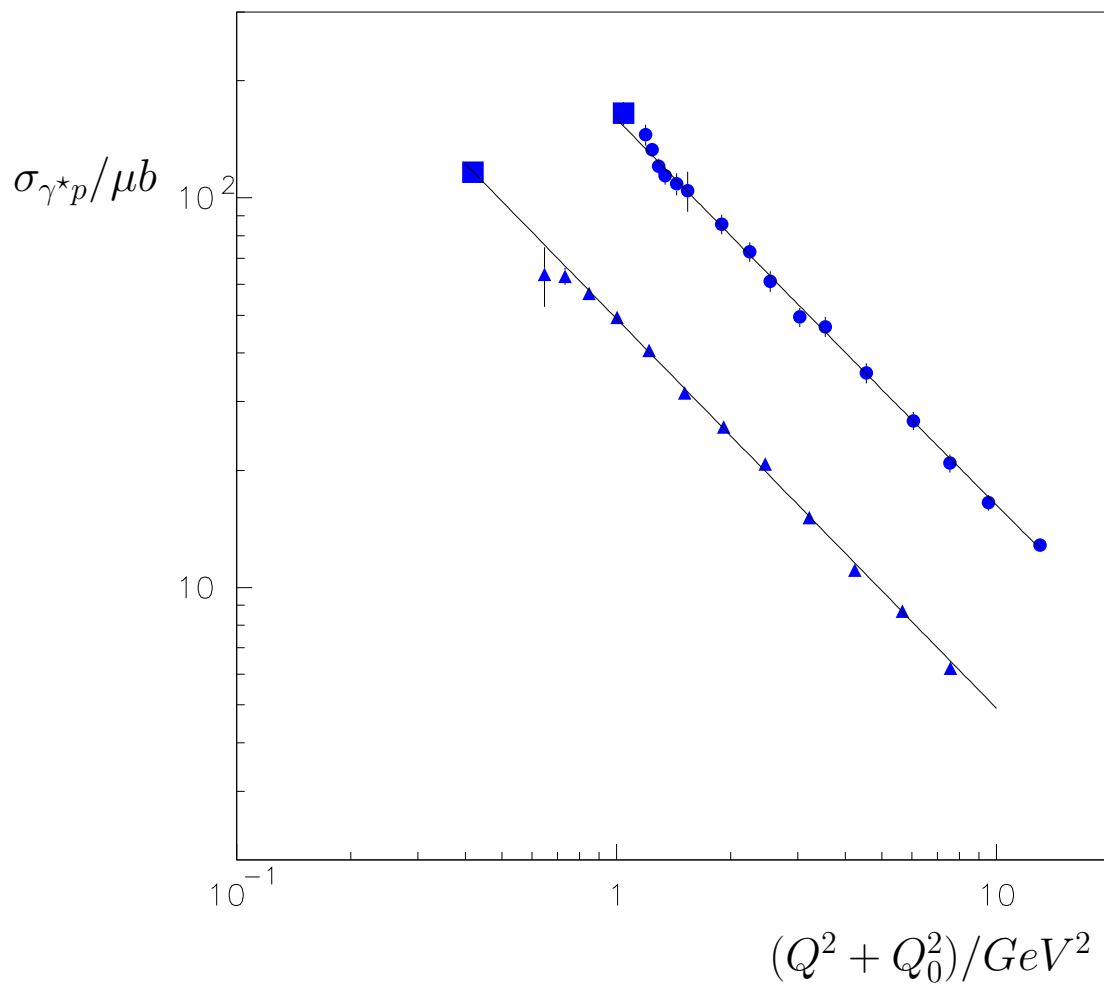


Figure 1

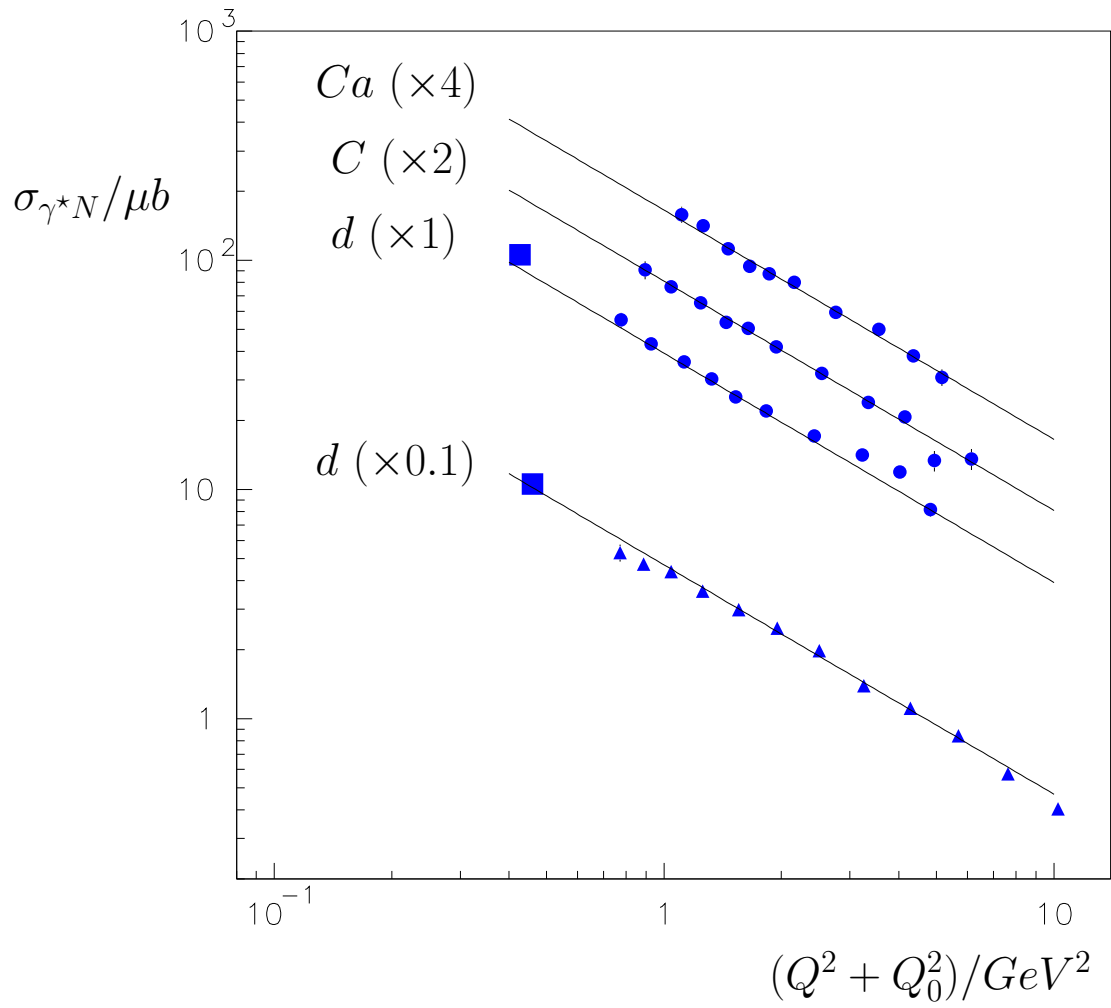


Figure 2